A comprehensive performance evaluation of bifacial photovoltaic modules: insights from a year-long experimental study conducted in the Canadian climate

Soufiane Ghafiri, Maxime Darnon, Arnaud Davigny, João Pedro F Trovão, Dhaker Abbes

EPJ Photovoltaics **15**, 28 (2024)

https://doi.org/10.1051/epjpv/2024025

Available online at:
www.epj-pv.org

ORIGINAL ARTICLE OPEN ACCESS

A comprehensive performance evaluation of bifacial photovoltaic modules: insights from a year-long experimental study conducted in the Canadian climate

Soufiane Ghafiri[1,2,3,*], Maxime Darnon[2], Arnaud Davigny[1], João Pedro F. Trovão[3], and Dhaker Abbes[1]

[1] L2EP, University of Lille, Arts et Metiers Institute of Technology, Centrale Lille, Junia, ULR, Lille, France
[2] Laboratoire Nanotechnologies Nanosystèmes (LN2) – CNRS UMI-3463 Institut Interdisciplinaire d'Innovation Technologique (3IT), Université de Sherbrooke, Sherbrooke, Québec, Canada
[3] e-TESC Lab, Université de Sherbrooke, Sherbrooke, Québec, Canada

Received: 14 November 2023 / Accepted: 29 July 2024

Abstract. Bifacial photovoltaic (PV) modules, capable of capturing solar energy from both sides of the cells, are becoming increasingly popular as their manufacturing costs approach those of traditional monofacial modules. Accurate estimation of their power generation capacity is essential for optimizing their use. This study evaluates a power production model for bifacial PV modules using local irradiance data from Razon+ in Sherbrooke, Canada, and Solcast irradiance data derived from satellite imagery and weather models. The model's performance was assessed throughout the year, with particular attention to the impact of snow coverage during winter. To address computational efficiency, the study evaluated ray tracing and a 2D view factor model, selecting the more time-efficient method. Experimental validation showed that, using local irradiance data, the model achieved Normalized Root Mean Square Errors (NRMSE) of 18.77%, 4.94%, 3.93%, and 6.22% for winter, spring, summer, and fall, respectively. With Solcast data, the NRMSEs were 22.76%, 15.32%, 14.72%, and 17.78% for the corresponding seasons. While the model performed satisfactorily in spring, summer, and fall, it was less accurate in winter. To enhance winter accuracy, the model incorporated snow coverage, using snow depth as a metric to detect snow on the front surface. This adjustment improved the accuracy by 51.1%.

Keywords: Photovoltaic / bifacial PV panels / power model / raytracing technique / view factor approach / snow losses

1 Introduction

It has been reported in the literature that the use of bifacial panels can improve the energy yield of power plants by 25–30% [1]. Due to their promising efficiency, bifacial panels have been widely deployed in a variety of applications, such as green roofs, agriculture and highways [2–6]. The rated power of bifacial modules is not straightforward to define, since it depends on various factors, such as the nature of the ground, the mounting configuration, and the bifaciality factor. The higher this factor is, the higher the module output power. Current PERC cells' bifaciality factors measure at 0.7, with SHJ cells exhibiting the highest values of up to 0.92 [7]. Accurate estimation of the energy production of photovoltaic (PV) modules is a crucial part of achieving optimal system sizing [8], as evidenced by a high-Performance Ratio (PR). A study [9] has demonstrated that ignoring soiling effects in the region, PR can be reduced by up to 26%. Furthermore, the validity of this statement was reinforced by [10], which indicated that the monthly losses due to snow coverage in severe climates can reach as high as 100% which reduces significantly the system's performance ratio. Numerous studies have delved into the effects of snowfall on monofacial photovoltaic (PV) modules. For instance, the authors of one such study [11] discovered that energy losses in PV systems due to snow accumulation could reach up to 90% on a monthly basis and fluctuate between 1% and 12% annually. A comprehensive review [12] paper further corroborates these findings, indicating that while annual electricity generation losses were generally less than 10% in most climates, monthly losses during winter months typically exceeded 25%. Bifacial PV panels, on the other hand, present a unique advantage. They are capable of producing an additional 10–15% of electrical energy by harnessing reflected light from the ground [13], This capability is particularly pronounced

* e-mail: ghas2002@usherbrooke.ca

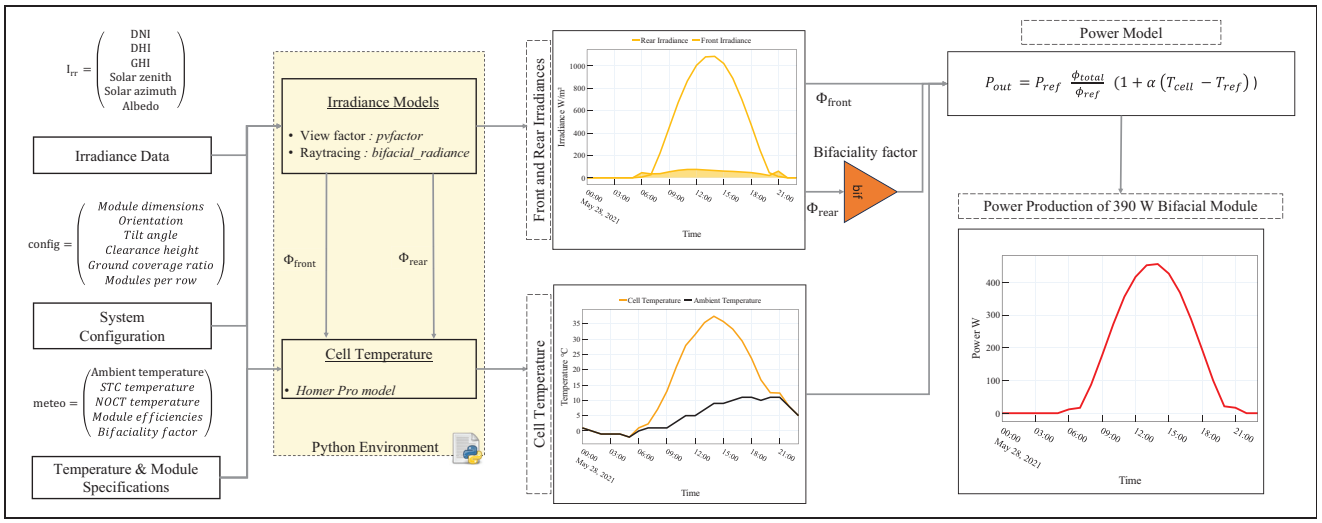

Fig. 1. Model for the power production estimation.

when the albedo is high due to snow cover. This distinctive feature enables bifacial PV panels to recover more swiftly from snowfall events and resume normal operation. In contrast, monofacial PV panels may remain obstructed by snow for extended periods.

Recent studies have examined the accuracy of predicting power production from bifacial solar panels utilizing various methods, such as view factors and the ray-tracing technique. Results demonstrated high accuracy in comparison to field measurements. In [14], a simple model was proposed to consider received irradiance and module temperature. The authors reported an 8% maximum residual error. Validation of this model was conducted with 25 days' data, the model displaying an overestimation of power at higher temperatures. In [15], a model based on the configuration factor was introduced, which calculations focused solely on back-side irradiance. This model was validated using data from a 6-month period. In [16], an electro-thermal model was proposed to assess the energy yield of bifacial modules and their dependence on parameters such as albedo. It was reported that a ground albedo of 0.5 could increase the global bifacial gain by about 20%. To eliminate the effects of snowing, only data from 3 months was used for validation. The purpose of [17] is to evaluate the performance of a range of irradiance tools, by assessing their predictions against measurements. In particular, it was shown that the bifacial gain for Fixed-Tilt systems varied between 5.5% and 7.5%, compared with an experimental result of 6%.

This research work differs from previous studies by three significant contributions to the field of bifacial photovoltaic (PV) modules. Firstly, it introduces a power model for bifacial PV modules, capable of estimating power output based on various factors such as irradiance on the front and rear surfaces, cell temperature, and more. Secondly, the model is validated through a year-long experiment involving 12 bifacial PV modules installed at Université de Sherbrooke in Canada. The validation process involves a comparison of the model's results with measured data, evaluated using metrics like the normalized root mean square error (NRMSE) and bifacial gain. Lastly, the authors conduct a sensitivity analysis of the model, examining its response to different sources of weather data and reducing the probability of overestimating the power production by considering the impact of snow coverge.

2 Methodology

The power model of the bifacial module is presented in Figure 1. It is a model that employs two different approaches to estimate the module irradiance; either we can employ the view factor method by using *pvfactors* or the raytracing technique by using *bifacial_radiance*. The module bifaciality coefficient is then multiplied by the rear irradiance and added to the front irradiance. The cell temperature is computed using Homer Pro model. By selecting the irradiance model presented in [18] carefully, one may choose between accuracy and execution speed. For example, *bifacial_radiance* can be used to analyze the irradiance on a specific segment of the module, the influence of the torque tube, or the nature of the ground on panel production. *pvfactors*, on the other hand, enables quick simulations. The power equation of the bifacial module is expressed as:

$$P_{bif} = P_{mp} \frac{\left(\Phi_f + \eta \Phi_r\right)}{\Phi_{ref}} \left(1 + \alpha_p \left(T_{cell} - T_{c,stc}\right)\right)(1 + D) \tag{1}$$

where η is the bifaciality factor, ϕ_r[W/m^2] and ϕ_f[W/m^2] are the rear and front irradiance respectively, α_p: temperature coefficient of power, Φ_{ref}: reference irradiance, P_{mp}: module maximum power, $T_{c,stc}$: cell temperature at STC, T_{cell}: module cell temperature, and D is the derate coefficient. The cell temperature of the PV module is

(a) Installed PV Array on the UdeS Campus

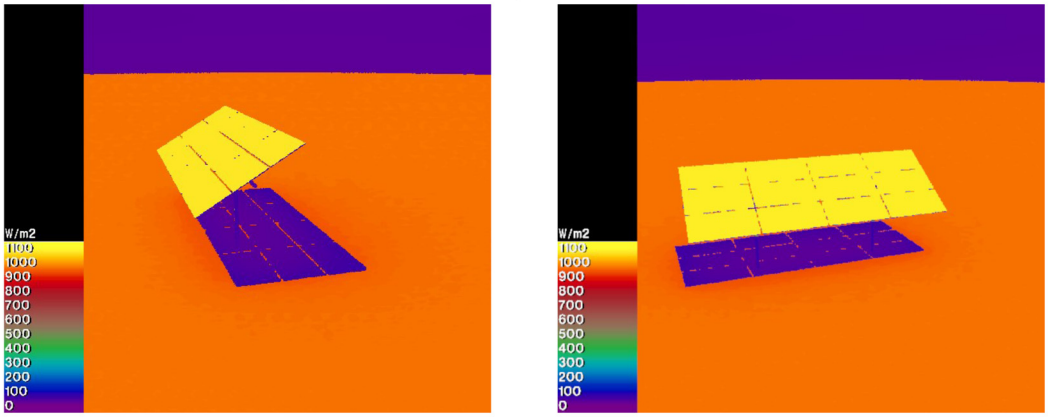

(b) Ray Tracing Technique Applied to PV Array: Side View (Left) at 13:00 on 2021-05-28 and Front View (Right) at 14:00 on 2021-05-28

Fig. 2. Raytracing Technique applied to UdeS PV Array.

critical for estimating the power production of the module. The equation used by Homer Pro for estimating the cell temperature is [19]:

$$T_{cell} = \frac{T_a + \left(T_{c,noct} - T_{a,noct}\right)\frac{\Phi_t}{\Phi_{t,noct}}\left(1 - \frac{\eta_{p,stc}(1-\alpha_T T_{cstc})}{\gamma\tau}\right)}{1 + \frac{\Phi_t\left(T_{c,noct} - T_{a,noct}\right)\alpha_T \eta_{p,stc}}{\Phi_{ref}\gamma\tau}} \tag{2}$$

where T_a: ambient temperature, $T_{c,noct}$: nominal operating cell temperature [C], $T_{a,noct}$ ambient temperature at which $T_{a,noct}$ is defenied, Φ_t total received irradiance, $\Phi_{t,noct}$ solar irradiance at which $T_{c,noct}$ is defined, $\eta_{p,stc}$: maximum power efficiency under standard test conditions [%], α_T: temperature coefficient [%/C], τ: solar transmittance [%], and γ: solar absorptance [%]. The Homer model sets the value of the product $\gamma\tau$ to 0.9, and the rest of the coefficients are obtained from the module's datasheet.

The Power production data of 12 PV modules (Fig. 2) was collected from Université de Sherbrooke for all seasons of the year 2021, this amount of data will be utilized to evaluate the model under varied weather conditions. The used system is composed of 12 modules mounted at 30° in landscape configuration. We used 390 W monocrystalline bifacial modules. The module are connected in a series configuration via SolarEdge power optimizers. These optimizers facilitate Maximum Power Point Tracking (MPPT), thereby optimizing the energy extraction from each individual module. Furthermore, they provide the capability to monitor the power and energy output of each module independently. The optimizers exhibit a weighted efficiency of 98.8%, with a peak efficiency reaching as high as 99.5%. The detailed system configuration is summarized in Table 1.

The RaZON+ system from Kipp and Zonen is employed to measure two key types of solar irradiance: Direct Normal Irradiance (DNI) and Diffuse Horizontal Irradiance (DHI). These measurements are crucial as they are used to calculate the Global Horizontal Solar Irradiance (GHI). For albedo values, we utilize data provided by Solcast. This data is derived from NASA's Moderate Resolution Imaging Spectroradiometer (MODIS) products, which offer historical albedo data. To cater to specific locations and times, the data undergoes spatial and temporal interpolation. Solcast ensures the accuracy and

Table 1. System mounting parameters of the modules.

Parameter	Value
Module type	LG390N2T-A5
Cell Type	Monocrystalline / N-type
Bifaciality Coefficient	76
Tilt Angle	30
Number of rows	1
Number of modules	12
Center Height	2.4 m
Surface Azimuth	180
Ground Coverage Ratio	0.001
Orientation	Landscape

consistency of this interpolated data by performing bias corrections. The solar Zenith and Azimuth angles is provided by the RaZON+ System, which calculates the solar angles using NREL's Solar Position Algorithm (SPA) [20]. This algorithm enables accurate tracking of the sun's position throughout the day. These parameters, collected on an hourly basis, serve as the foundation for the model depicted in Figure 1. The EdgeSolar Optimizer is employed to monitor the power output's hourly fluctuations. This data, representing the system's actual performance, is subsequently used as a benchmark to assess the model's precision. By comparing the model's predictions with these real-world measurements, we can evaluate the model's accuracy and make necessary adjustments to improve its predictive capabilities. In order to ensure the quality of our data, we have employed two distinct techniques. The first involves the removal of outliers by imposing limits on the parameter values. For instance, we have set the maximum value of the received irradiance equal to the constant solar irradiance, thereby eliminating any anomalously high readings. The second technique pertains to the handling of missing values. If any parameters required to estimate the power output are missing for a specific hour, we exclude that hour from our dataset. Consequently, our meteorological input data has been reduced from 8760 to 8676 entries, indicating that 84 values have been filtered out due to missing parameters.

3 Results and discussion

3.1 bifacial_radiance

The application of ray-tracing technique by the using *bifacial_radiance* [21], presents a significant challenge due to the extensive computational time required, which is not conducive to a comprehensive, hourly analysis over an entire year. In fact, a one-year simulation of our system is projected to require approximately 13 h of computation on a computer equipped with an Intel® Core™ i5-8265U CPU @ 1.60GHz 1.80 GHz and 8 GB of RAM. To address this issue, we employed code optimization in conjunction with parallel computing, which effectively reduced the execution time to a mere 3 hours. The strategy involves utilizing the measured data as input for the function responsible for calculating the hourly power production (specifically, the gendaylit2manual function in *bifacial_radiance*). The simulation of a single day is then decomposed according to the number of processors available in our machine. This approach allows for a more efficient use of computational resources, thereby significantly reducing the overall execution time.

As illustrated in Figure 2, we implemented the ray-tracing technique to the given scene, taking into account the mounting parameters of the system. To enhance precision, we configured the *bifacial_radiance* parameter to accommodate nine sensors. This configuration is based on the array's composition, which consists of three rows with four modules each, resulting in three sensors per module. The data acquired from this setup enabled us to conduct a comprehensive analysis of the system and ascertain the power output of each individual module. This rigorous approach ensures a detailed understanding of the system's performance. The Normalized Root Mean Square Error (NRMSE) (Eq. (3)) was computed for each individual module over a three-month period corresponding to each of the four seasons in the year 2021, as a measure to evaluate the precision of the power model and quantify its deviation from the experimental data. This error measurement is normalized by the range of the observed values, as shown in the equation below (Eq. (3)). The results are depicted in Figure 3.

$$NRMSE = \frac{\sqrt{\frac{1}{N}\sum_{i=1}^{N}\left(P_{meas,i} - P_{est,i}\right)^2}}{P_{meas,max} - P_{meas,min}} \tag{3}$$

where $P_{meas,i}$ and $P_{est,i}$ are the measured and the estimated energy in the hour i, and N number of a season days, $P_{meas,max}$ and $P_{meas,min}$ are the maximum and the minimum power respectively.

The summer season, with its higher number of clear sky days compared to other seasons, exhibits the lowest NRMSE values. The maximum value for this season is 4.7%, while the minimum value is 3.1%, indicating a commendable degree of accuracy for the model during this period. In the spring season, the NRMSE values range from 4.7% to 5.4%, which is still within an acceptable range. However, during the autumn season, there is a rise in the NRMSE values of each module, with the minimum value being 5.8% and the maximum value reaching 6.8%. The observed augmentation can be attributed to the amplified frequency of cloudy conditions prevalent during this particular season. This is evident from Table 2 showing the monthly fraction of cloudy days. As we analyze the data, we see that the monthly fraction of cloudy days rises from 52% to a significant 72% in December. However, the model's accuracy shows a notable variation during the winter season, with NRMSE values fluctuating between a minimum of 16.1% and a maximum of 19%. Despite the superior quality of the validation data, it's presumed that the main contributor to these significant NRMSE values is the snow coverage. This postulation is based on the

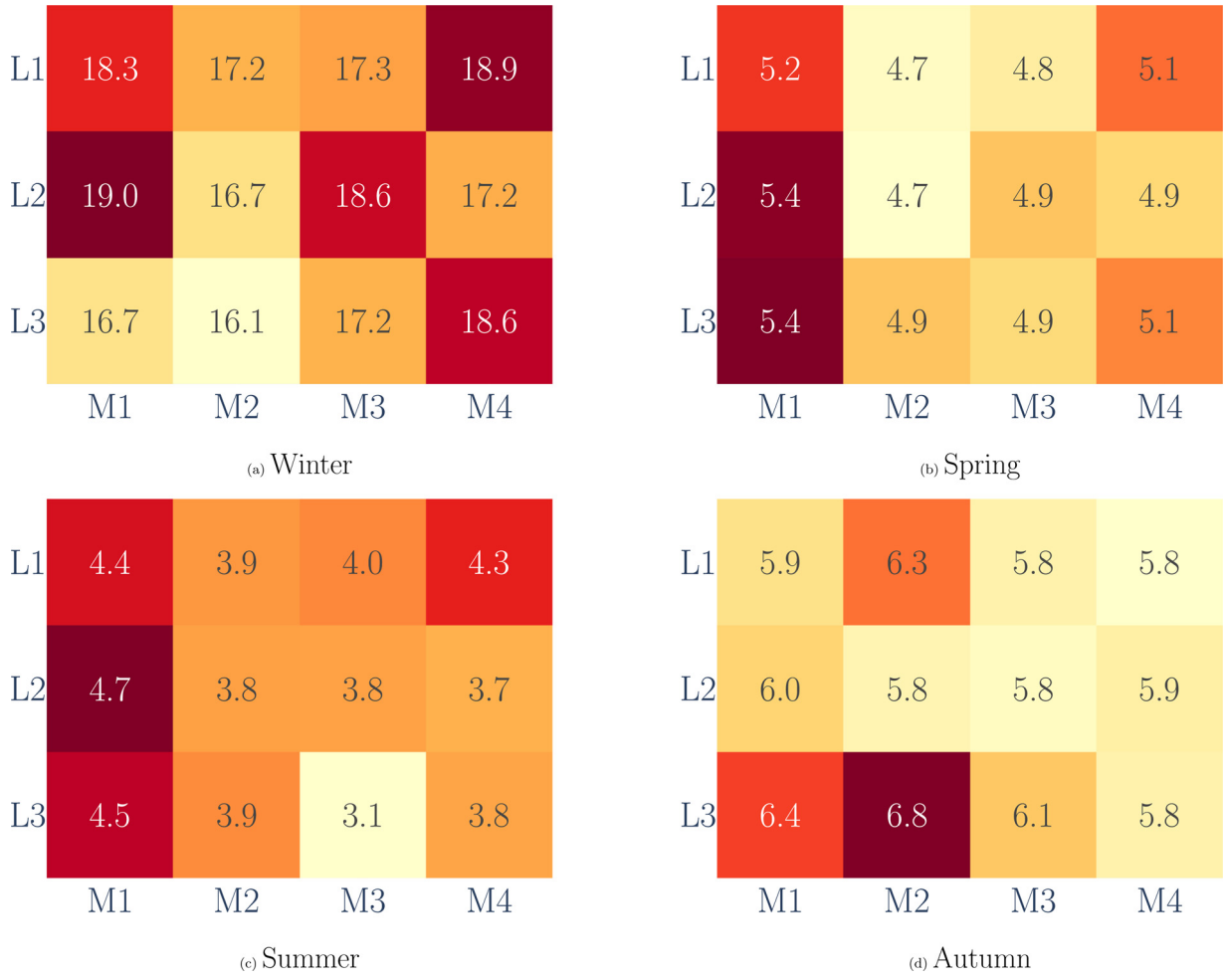

Fig. 3. Seasonal NRMSE [%] for the year 2021.

geographical location's tendency for winter snowfall, suggesting that the degree of snow coverage during the winter season has a substantial effect on the model's power production.

3.1.1 Seasonal bifacial gain

Snow albedo is the fraction of incoming light or radiation that a surface reflects. It ranges from 0.5 to 0.7 for old snow, but it can surpass 0.9 for freshly fallen snow [22]. As a result, in the winter, the received ground-reflected irradiance increases significantly, as does the bifacial gain. To quantify the additional energy obtained by using bifacial modules versus monofacial modules, we compute the bifacial gain, that represents the ratio of the irradiance received by the back surface to the irradiance received by the front surface. As expressed in the equation (4), we consider the efficiency of the module's backside. This equation is commonly used in the literature, and it is an approximation of the actual value.

$$G_{bif} = \eta \frac{\phi_r}{\phi_f} \tag{4}$$

where η is the bifaciality factor, ϕ_r[W/m^2] and ϕ_f[W/m^2] are the rear and front irradiance respectively.

Figure 4 illustrates the remarkable advantage of employing bifacial modules with our system configuration. These modules can boost efficiency by as much as 28.4% during winter months, a figure nearly three times the minimum improvement observed in summer, which stands at 9.8%. In terms of seasonal variations, the bifacial gain fluctuates between 8.4% and 10% in spring, 8.5% and 10.1% in summer, and 9.8% and 11.7% in autumn. The increase in autumn is attributable to the rise in albedo values. Upon closer examination, it is evident that the modules located at the bottom and in the center exhibit a lower gain compared to those at the top edges. This discrepancy can be attributed to the shading effect caused by the mounting structure and torque tube for the central modules, and the reduced rear side collection due to lower altitude for the bottom modules. It is important to note that the bifacial gain discussed here is based on modeling and does not account for snow losses. which are known to decrease when photovoltaic (PV) modules are bifacial [10].

Table 2. Monthly distribution of cloud cover and clear days: Data courtesy of WeatherSpark.com.

Fraction	Jan	Feb	Mar	Apr	May	Jun	Jul	Aug	Sep	Oct	Nov	Dec
Cloudier	75%	72%	66%	60%	57%	52%	43%	40%	43%	52%	64%	72%
Clearer	25%	28%	34%	40%	43%	48%	57%	60%	57%	48%	36%	28%

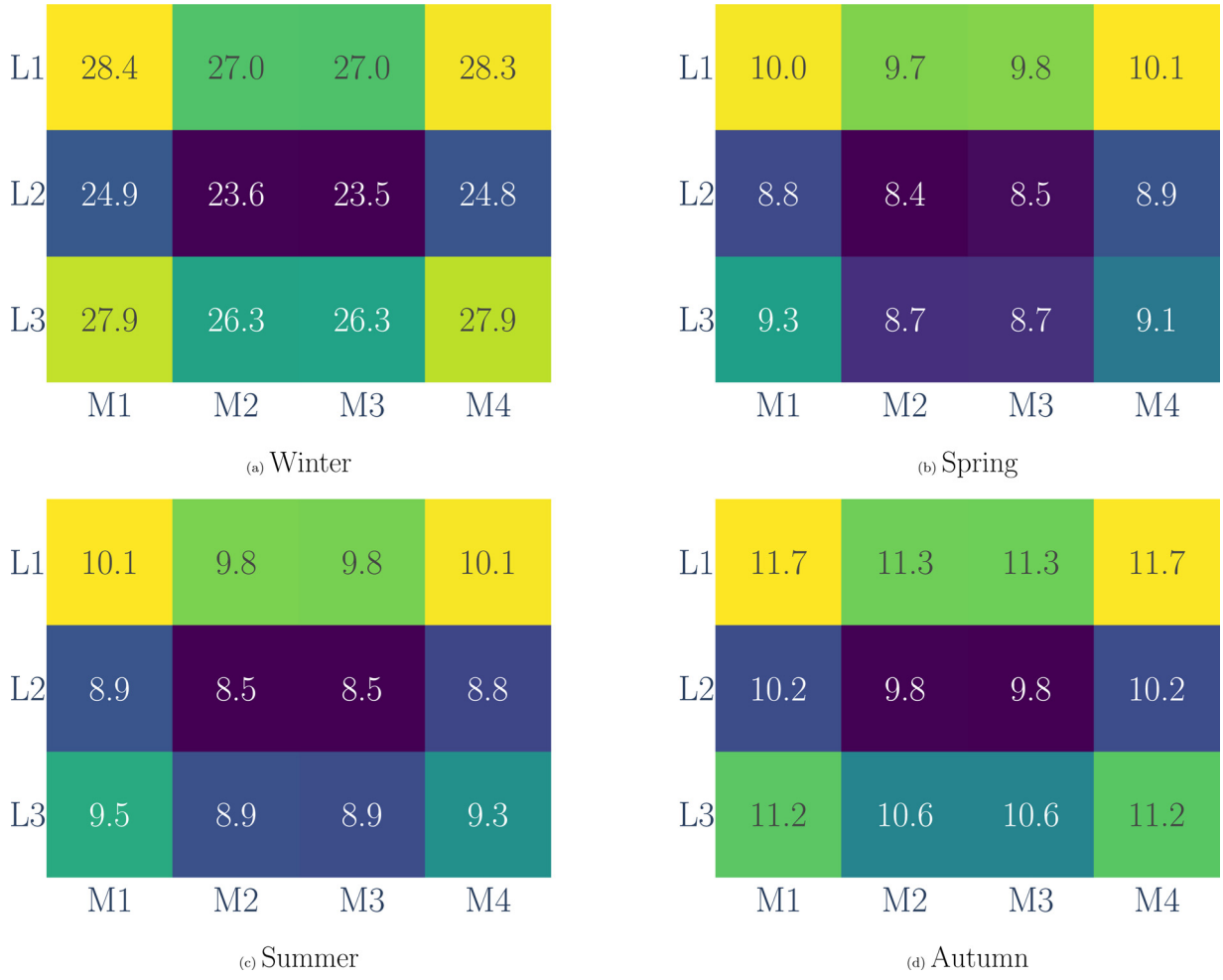

(a) Winter (b) Spring (c) Summer (d) Autumn

Fig. 4. Seasonal Bifacial Gain [%] of the year 2021 using bifacial radiance.

3.2 PV factors

A fast simulation can be reached using *pvfactors* [23]. *pvfactors* assumes that all the modules at the same altitude are similar (2D View Factor model). This assumption, however, limits the ability to study power production variations among adjacent modules with identical mounting properties. It is of significance to note that the Ground Coverage Ratio (GCR) delineated in Table 1 aligns with the value utilized for the *pvfactors* model. As *bifacial_radiance* model can accommodate a GCR value of 0. *pvfactors* operates as a view factor model, employing the GCR to compute the spacing required to achieve the desired GCR. This spacing is crucial for accurate modeling THE shading characteristics A GCR value of 0 would result in an error in this context. Consequently, to circumvent this issue, we approximate this value to 0.001.

To validate the model using *pvfactors*, we selected the modules located at the highest point and initiated a simulation spanning one year. Remarkably, the execution time for this simulation was a mere 15 seconds. This swift computation time is particularly advantageous for

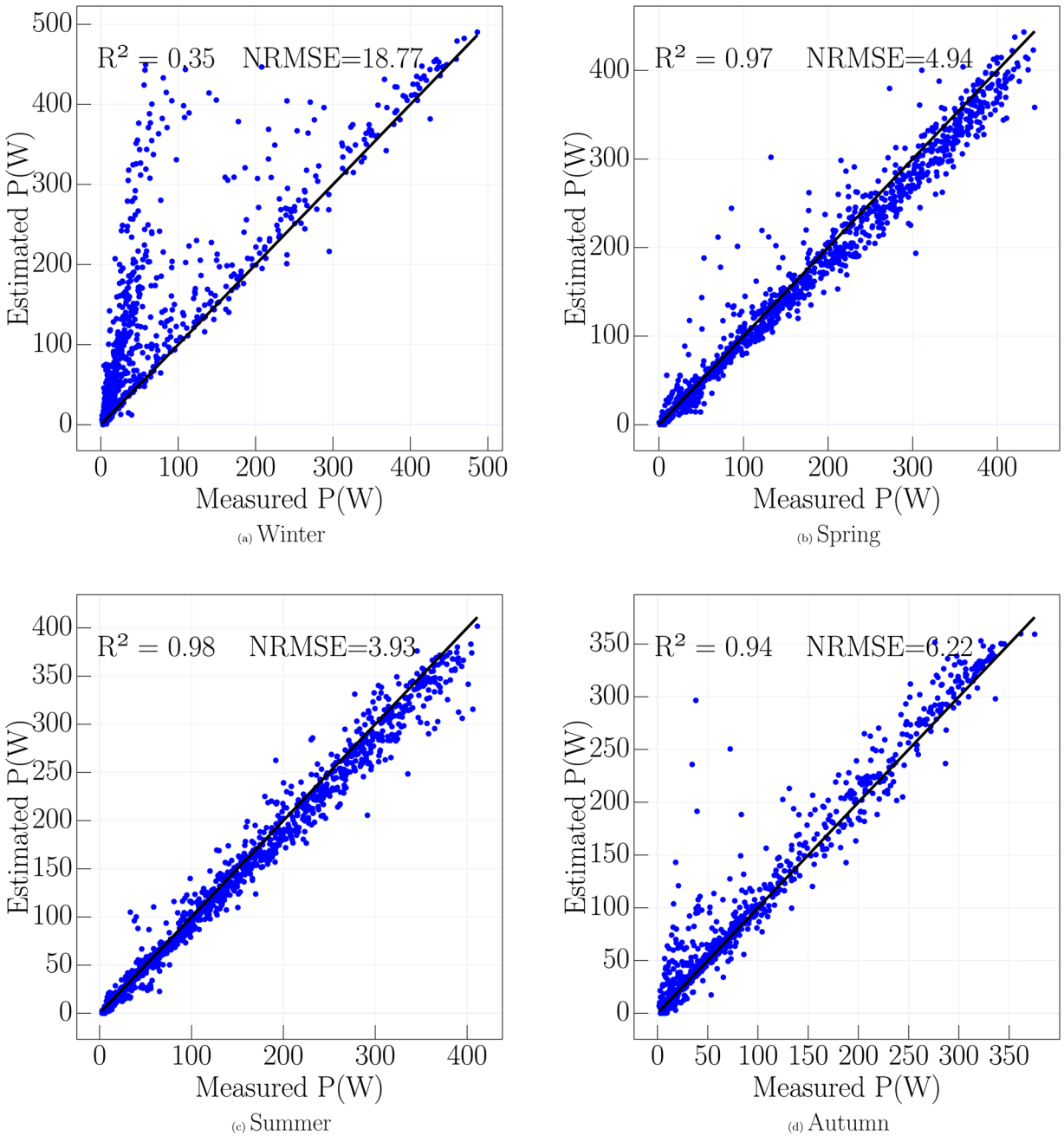

Fig. 5. Comparison of Measured and Estimated Power Output using pvfactors (Top Module) and local data with Razon+.

modeling larger scale photovoltaic (PV) systems or for integrating this model into simulations that necessitate multiple iterations.

The scatter plots depicted in Figure 5 illustrate a comparison between the hourly measured power and the estimated power using the *pvfactors* model. We compare the simulation output with the mean power production of the top four modules. Similarly to modeling with *bifacial_radiance*, the PV production is overestimated during the winter season. This overestimation is attributed to the snow effect. The Normalized Root Mean Square Error (NRMSE) peaks at 18.77%, and the coefficient of determination (R^2) is 0.35. This suggests that the model moderately fits the experimental data, leaving 65% of the variability unexplained. However, the model aligns well with the measured values during the spring and summer seasons. This is evidenced by the coefficients of determination of 0.97 and 0.98 respectively, and NRMSE values of 4.94% and 3.93%. A minor deviation is observed during the autumn season, with an error of 6.22% and a coefficient of determination of 0.94. This deviation can be associated with the occasional snowy days characteristic of this season, particularly in December.

Table 3. Results of the simulation using *pvfactors* and *bifacial_radiance*.

		Pvfactors	Bifacial_radiance
Bifacial Gain			
	Winter	33.11	27.67
	Spring	13.54	9.9
	Summer	13.97	9.95
	Autumn	14.58	11.5
NRMSE %			
	Winter	18.77	17.92
	Spring	4.94	4.90
	Summer	3.93	4.12
	Autumn	6.22	5.96
Excution Time		15 seconds	3 hours

The performance of the two modeling methods in terms of two factors (Error and execution time) is compared in Table 3. We notice that *pvfactors* has almost the same values as *bifacial_radiance* except for the computation time. The model with *pvfactors* shows therefore an interesting advantage for integration into management strategies and optimization problems for hybrid systems or microgrids that require multiple iterations. However, it is not capable of capturing 3D effects such as the impact of the mounting structure that was clearly visible with *bifacial_radiance*.

3.3 Sensitivity analysis

In this section, we examine the sensitivity of the model with respect to input data. As previously noted in Section 2, validation of the model was conducted using measured data, except for the albedo parameter. Therefore, this section addresses the accuracy of the model when it is supplied exclusively with weather data obtained from Solcast, which utilizes geostationary weather satellites and weather model data to estimate irradiance components. Various satellite-derived solar irradiance datasets provide historical irradiance time series, such as SOLARGIS, PVGIS, Solar AnyWhere, and METEONORM. Among these, Solcast stands out due to its promising characteristics, including its remarkable precision, which has been demonstrated in the publication [24].

The performance of the model utilizing Solcast irradiation data is detailed in Figure 6, with each subfigure representing a specific season in the year 2021. Significant errors are observed across all seasons. Even in summer, which typically experiences the clearest skies (Tab. 2), the Normalized Root Mean Square Error (NRMSE) is 14.72%, with a coefficient of determination (R^2) of 0.71. During spring, the NRMSE is 15.32% with an R^2 of 0.71, while autumn exhibits an NRMSE of 17.78% and an R^2 of 0.55. As anticipated, winter shows the highest error and greatest discrepancy between measured and estimated values, with an NRMSE of 22.76% and an R^2 as low as 0.07.

The elevated error values are attributed to the input data quality. To investigate this, we compared Solcast's historical data with measured data, focusing on four primary parameters impacting power production estimation: DNI, DHI, GHI, and Temperature. We computed the NRMSE for each parameter, summarized in Figure 7. The NRMSE values for DNI, DHI, GHI, and Temperature were 36.81%, 24.03%, 30.12%, and 12.81%, respectively.

3.4 Impact of snow coverage

This paper underscores the impact of snow on the energy yield of bifacial panels, a factor that significantly influences the sizing of power systems that utilize these panels. The common sizing methodology employs weather data, predominantly irradiance time series, to project the annual power variation of a single bifacial PV module. Subsequently, an optimization algorithm is used to ascertain the ideal number of modules needed to fulfill specific objectives while complying with load constraints. This method is extensively adopted in various studies and tools, including but not limited to Homer Pro and Pvsyst [25–27]. However, in regions prone to heavy snowfall, the power production of PV panels can be considerably diminished due to snow coverage.

To confirm the accumulation of snow on the modules, we have utilized the 'snow on the ground' metric, measured in centimeters. The variations in this specific parameter have been derived from an extensive database managed by a station located in Linexoville, Sherbrooke. In order to validate the presence of snow on the front surface of the module, we have strategically placed a camera directed towards the installed bifacial module. This configuration allows us to visually confirm and track the build-up of snow.

From Figures 8 and 9, a discernible pattern emerges: when the accumulated snow on the ground reaches or exceeds 2 cm, and the derivative of snow accumulation from the previous day is positive, the solar modules become entirely covered by snow on their front surface. This phenomenon is evident in the data for the four specific days depicted in Figure 9 namely, January 20, 2024, January 15, 2024, January 8, 2024, and May 12, 2024.

Conversely, it is observed that when the snow accumulation surpasses or equals 2 cm, and the derivative of the accumulation from the preceding day is negative, coupled with a significant temperature escalation, these conditions instigate the activation of the sliding phenomenon. This results in the clearance of the front surface of the bifacial panels. In our photographic series 35, we have documented a day where this phenomenon was observed, specifically on December 10th. On this day, the snow depth was 13 cm, however, there was a notable increase in the daily mean temperature. Starting from December 6th, 2024, the temperature rose from −10 °C and reached 5.5 °C on December 10th, 2024. This thermal shift appears to have contributed to the observed sliding phenomenon.

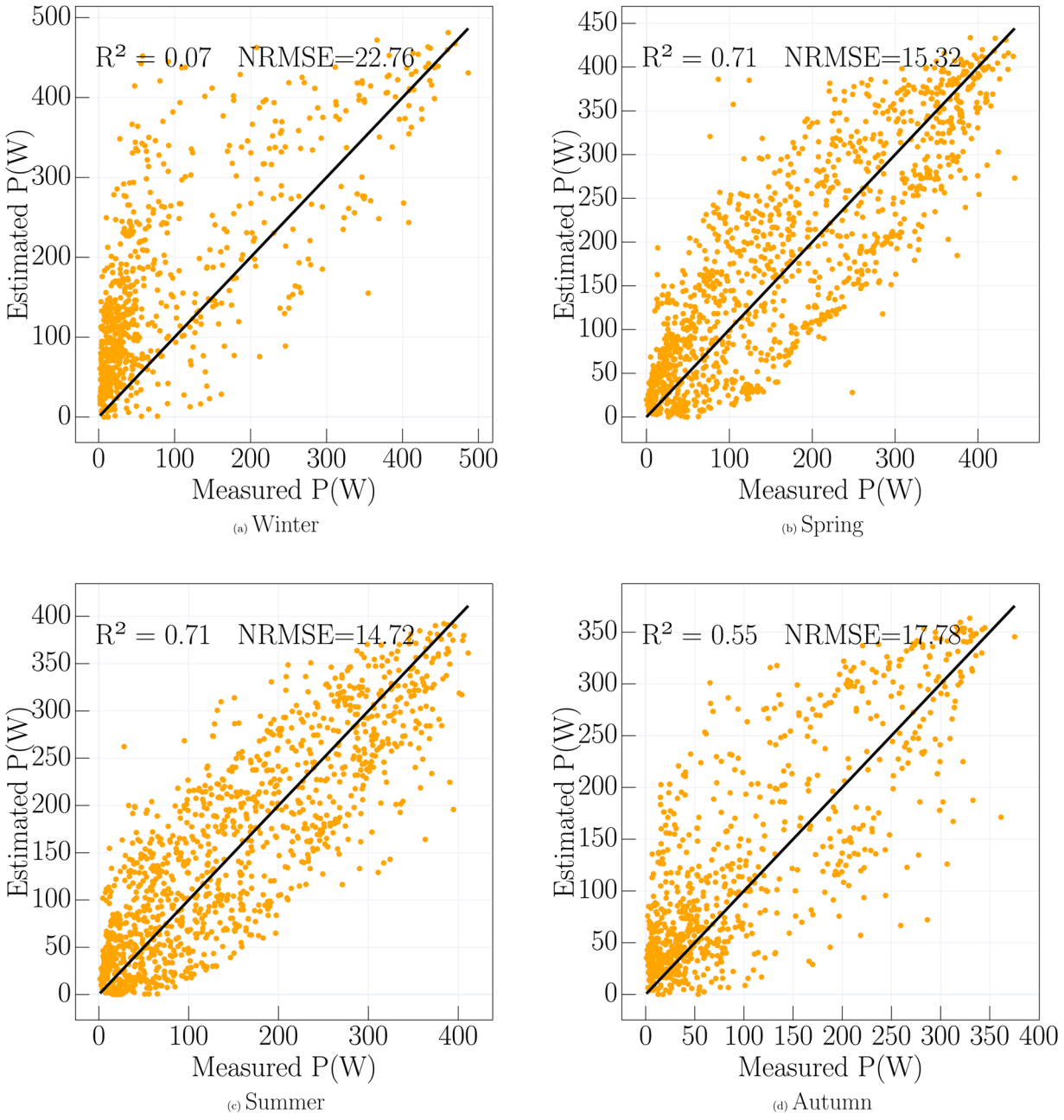

Fig. 6. Comparison of Measured and Estimated Power Output using pvfactors (Top Module) and Solcast Data.

Under the full coverage of the front surface all the string of the bifacial panels are masked with the snow. Thus only the rear surface of the bifacial modules generates the power based on the power and the expression of the power production can be expression as follows:

$$P_{bif} = P_{mp}\frac{\eta\Phi_r}{\Phi_{ref}}\left(1+\alpha_p\left(T_{cell}-T_{c,stc}\right)\right). \quad (5)$$

Figure 10 presents a heatmap of the production output for each module, recorded at 12:00 (UTC-5) on January 8, 2024. As depicted in Figure 8, the panels were entirely covered with snow throughout the day. The snow accumulation on the ground was measured to be 10 cm. In the absence of snow coverage, the top modules were estimated to produce approximately 86.6 W. However, the highest observed value was only 17.8 W, indicating a power loss of 79%.

To enhance the modeling of power production during the winter season, we employed equation (2) under conditions of complete snow coverage. We identified days where the snow depth exceeded 2 cm, and the daily mean and maximum temperatures were strictly below 0 °C to ensure the absence of snow sliding phenomena. These conditions were met from January 19, 2021, to February 27, 2021, and again from December 6, 2021. Previously, the

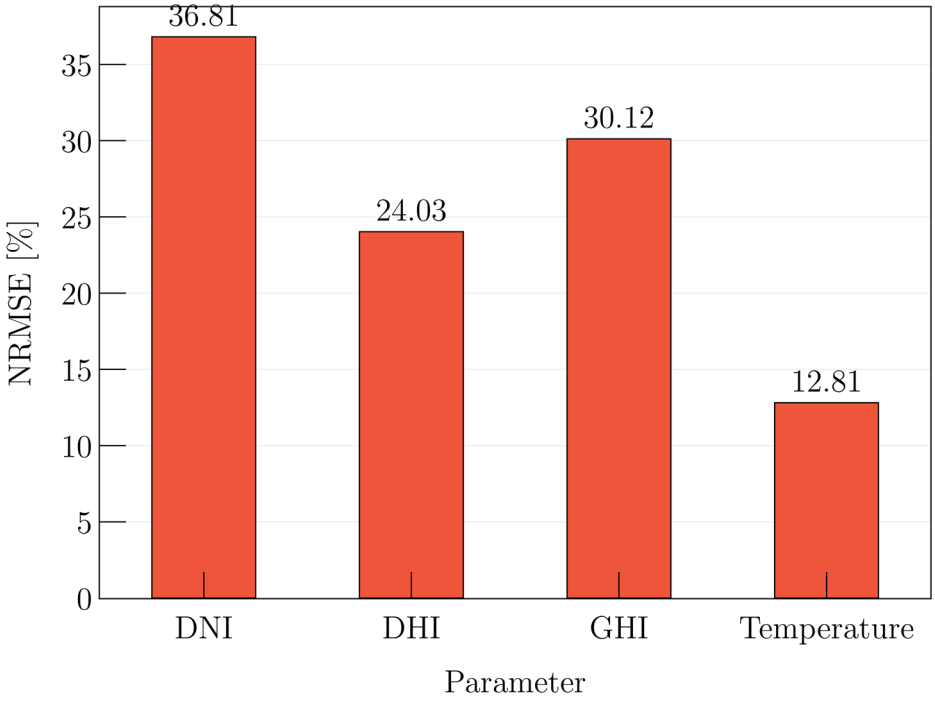

Fig. 7. Discrepancy between measured values and Solcast (Satellite-Derived): DNI, DHI, GHI, and Temperature.

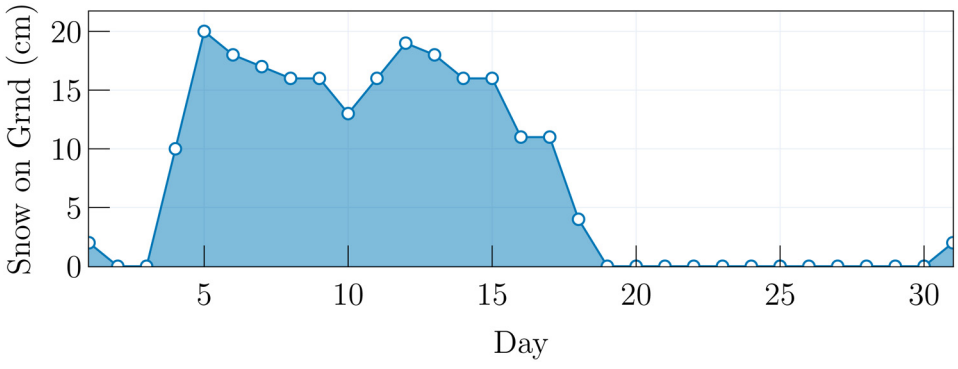

(a) December 2023

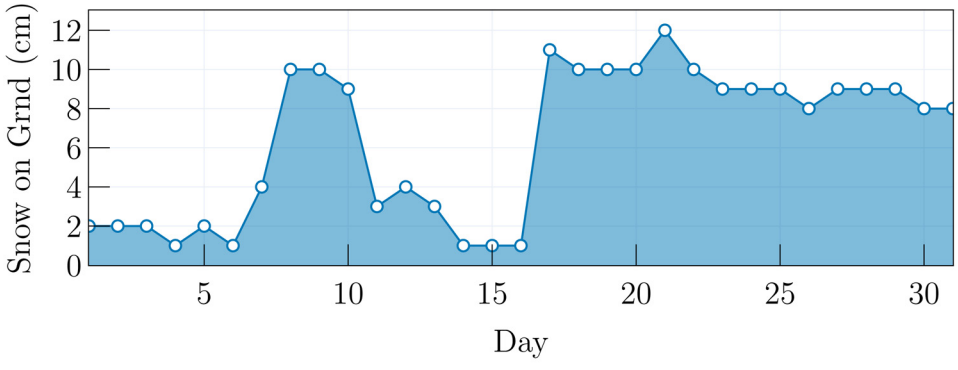

(b) January 2024

Fig. 8. Accumulation of snowfall (in cm) in Sherbrooke.

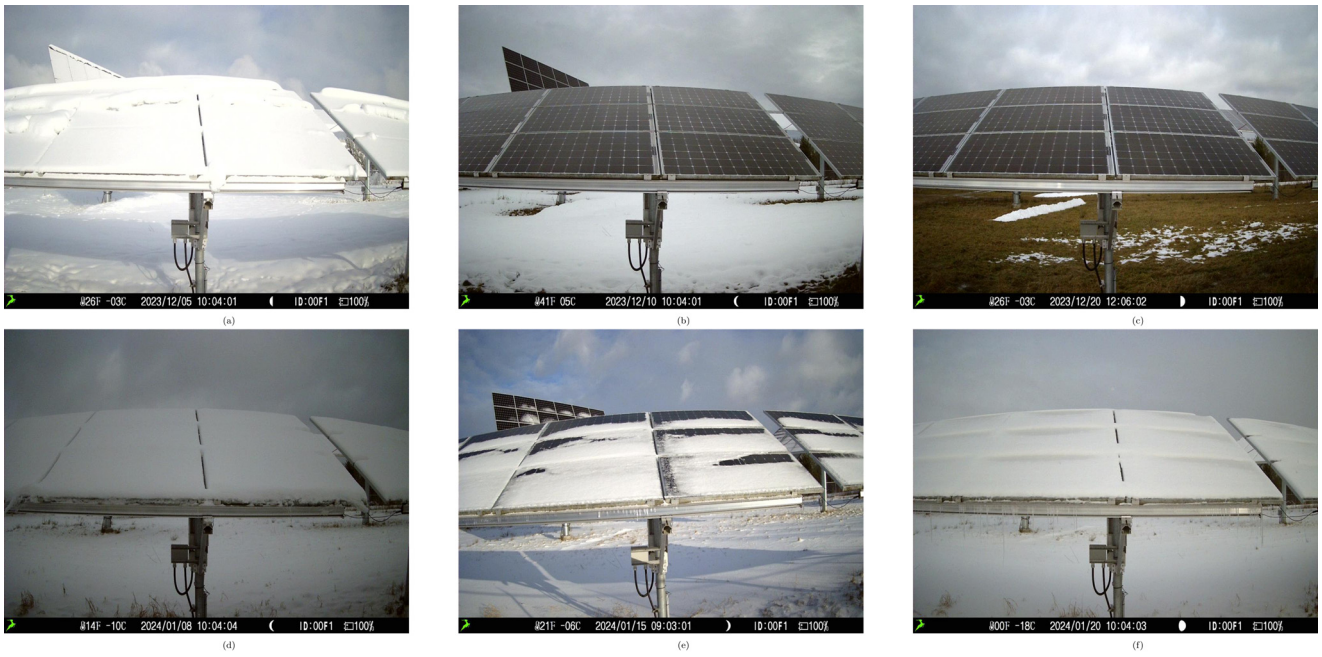

Fig. 9. Bifacial PV String Installation on Sherbrooke Campus: A photo series captured across selected Winter days of 2023-2024.

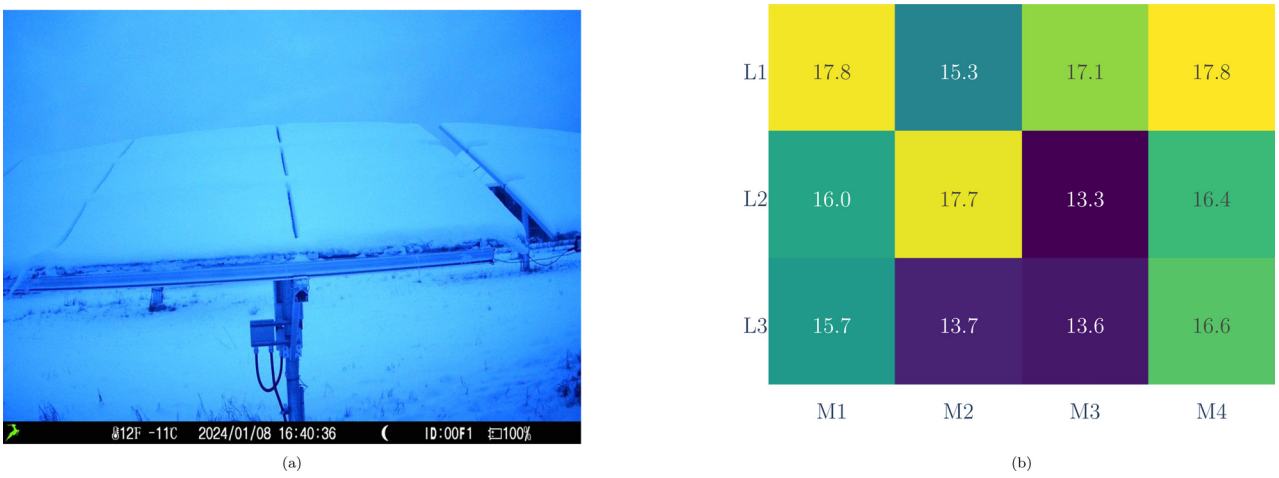

Fig. 10. Measured Power Output of fully snow covered front surface Bifacial Modules on January 8, 2024.

NRMSE value for the winter season was 18.77%, with an R^2 value of 0.35. After refining the modeling approach to account for the impact of snow, the NRMSE value improved to 9.17%, and the R^2 value increased to 0.83, reflecting an improvement of approximately 51.1% in NRMSE and a substantial enhancement in R^2.

Despite these improvements, further refinement is possible. As observed in Figure 11, there are instances where the power production of bifacial modules is underestimated. This discrepancy may be attributed to undetected snow sliding phenomena.

4 Conclusion

With their promising energy yield and reasonable manufacturing cost, bifacial panels technology is showing remarkable momentum in the PV market, thus an accurate and fast model of the bifacial panel is necessary for sizing and implementing efficient management strategies for stations that use these modules. This study presents an experimentally validated model of bifacial panels tailored for snow-prone climates, ensuring strict time efficiency.

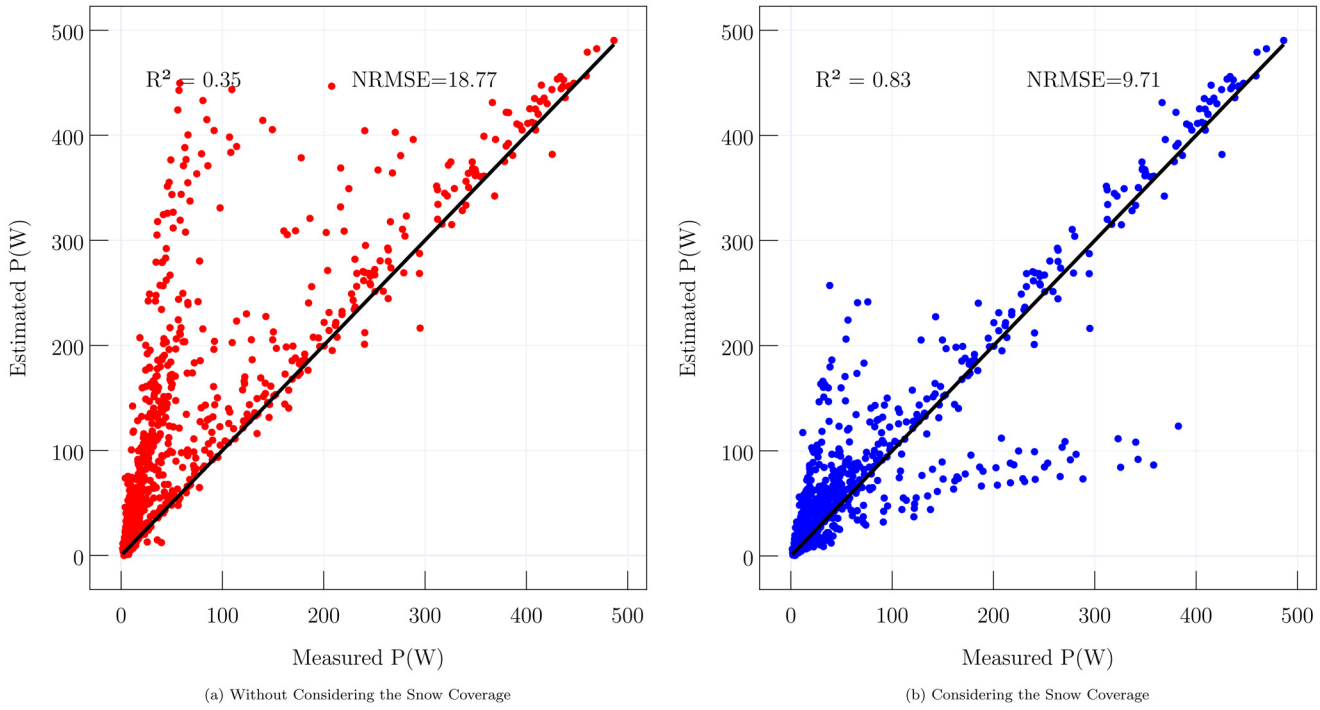

Fig. 11. Refinement of NRMSE value via snow coverage consideration in Winter season modelling.

The evaluated model, based on the *pvfactors*, achieves NRMSE of 18.77%, 4.94%, 3.93%, and 6.22% for Winter, Spring, Summer, and Fall, respectively. Remarkably, it accomplishes these results in under 15 seconds for a full year simulation of 2021. In contrast, simulations using the *bifacial_radiance* model are significantly slower, with corresponding NRMSE values of 17.92%, 4.9%, 4.12%, and 5.96% for the same seasons. The *pvfactors* model strikes a commendable balance between accuracy and execution time across three seasons, with winter being the exception. During winter, the model tends to overestimate power production due to high agreement with clear weather periods, leading to notable discrepancies. Sensitivity analysis using satellite-imagery driven data from Solcast revealed a substantial performance drop, attributed to the data quality. Further investigation, including camera monitoring of the PV arrays, identified snow coverage on the front surface of the modules as the primary cause of poor winter performance. Snow coverage can reduce production by up to 80%, leaving the rear surface as the sole power producer. Incorporating snow depth metrics to estimate snow presence on panel surfaces improved model accuracy by 51%. In summary, the *pvfactors*-based model offers a robust and efficient solution for simulating bifacial panel performance, particularly under varying seasonal conditions, while highlighting areas for improvement in snow-affected regions.

Acknowledgments

We would like to express our gratitude to all organizations that contributed to this research. We thank the Canada Research Chairs Program, the Natural Sciences and Engineering Research Council of Canada – NSERC, Bell and STACE for their partial funding and support of the SAFE-TELECOM project. We also acknowledge LN2, a collaborative International Research Laboratory jointly operated by Université de Sherbrooke, Canada, and CNRS, Ecole Centrale de Lyon, INSA Lyon, and Université Grenoble Alpes, France. We also thank The Fonds de Recherche du Québec Nature et Technologie (FRQNT) for providing financial assistance to LN2. We thank the Hauts-de-France region for its generous sponsorship. We appreciate the feedback and suggestions from the reviewers and editors of this journal.

Funding

The funding of this research was provided by several sources. The Canada Research Chairs Program (Grant 950-230672) awarded a grant to the corresponding author to conduct this research. The Natural Sciences and Engineering Research Council of Canada – NSERC (ALLRP558371-20) also supported this research as part of the SAFE-TELECOM project. Prompt (project 144), Bell and STACE are industrial partners of the SAFE-TELECOM project, and they provided technical and financial support to this research. LN2 is an international research laboratory that focuses on nanotechnologies and nanosystems, and it provided access to its facilities and equipment for this research. The Fonds de Recherche du Québec Nature et Technologie (FRQNT) is a provincial funding agency that supports LN2. The Hauts-de-France region is a regional authority in France that sponsored this research as part of its innovation policy.

Conflicts of interest

The authors declare that they have no known competing financial interests or personal relationships that could have appeared to influence the work reported in this paper.

Data availability statement

The data that support the findings of this study are not publicly available due to some confidentiality agreements with the industrial partners. However, the data can be accessed upon request from the corresponding author, who will provide the necessary information and instructions for obtaining the data. The data are stored in a secure online repository that requires a password and a permission from the author. The data are also subject to some ethical and legal restrictions that must be respected by the potential users.

Author contribution statement

The authors collaborated to develop the theoretical and modeling framework and the concept of the study. S. Ghafiri, A. Davigny, M. Darnon, J.P. Trovao and D. Abbes were the leading contributors in this aspect. M. Darnon also designed and conducted the experiment, and provided the input data for validating the model. S. Ghafiri was responsible for implementing the model in code and performing the data analysis and simulations. All authors participated in reviewing and revising the manuscript and agreed on the final version.

References

1. J. Stein, C. Reise, J. Castro, G. Friesen, G. Maugeri, E. Urrejola, S. Ranta, Bifacial photovoltaic modules and systems: Experience and results from international research and pilot applications (2021). https://doi.org/10.2172/1779379
2. M.S. Mahmud, M. WazedurRahman, M.H. Lipu, A.A. Mamun, T. Annur, M.M. Islam, M.M. Rahman, M.A. Islam, Solar highway in bangladesh using bifacial pv, In *2018 IEEE International conference on system, computation, automation and networking* (IEEE, 2018), pp. 1–7. https://doi.org/10.1109/ICSCAN.2018.8541253
3. M.H. Riaz, H. Imran, R. Younas, N.Z. Butt, The optimization of vertical bifacial photovoltaic farms for efficient agrivoltaic systems, Sol. Energy **230**, 1004 (2021). https://doi.org/10.1016/j.solener.2021.10.051
4. A. Martin, P.-P. Grand, M. Hull, J. Rousset, L. Oberbeck, Architecture of symmetrical bifacial perovskite/si/perovskite pv modules and lcoe comparison in bifacial applications, EPJ Photovolt. **14**, 33 (2023). https://doi.org/10.1051/epjpv/2023025
5. O.A. Katsikogiannis, H. Ziar, O. Isabella, Integration of bifacial photovoltaics in agrivoltaic systems: a synergistic design approach, Appl. Energy **309**, 118475 (2022). https://doi.org/10.1016/j.apenergy.2021.118475
6. T. Baumann, H. Nussbaumer, M. Klenk, A. Dreisiebner, F. Carigiet, F. Baumgartner, Photovoltaic systems with vertically mounted bifacial pv modules in combination with green roofs, Sol. Energy **190**, 139 (2019). https://doi.org/10.1016/j.solener.2019.08.014
7. F. Markus, H. Michael, W. Susanne, T. Jutta, International technology roadmap for photovoltaic 2022, ITRPV-VDMA, Tech. Rep. (2021)
8. M.H.O.P. Filho, V.A. Teixeira, Low cost electroluminescense lab implementation, in *IEA SHC International Conference on Solar Heating and Cooling for Buildings and Industry 2019* (ISES SWC, 2019), pp. 1–7. https://doi.org/10.18086/swc.2019.16.06
9. B. Decker, U. Jahn, Performance of 170 grid connected pv plants in northern germany – analysis of yields and optimization potentials, Sol. Energy **59**, 127 (1997). https://doi.org/10.1016/S0038-092X(96)00132-6
10. R.E. Pawluk, Y. Chen, Y. She, Photovoltaic electricity generation loss due to snow – a literature review on influence factors, estimation, and mitigation, Renew. Sustain. Energy Rev. **107**, 171 (2019). https://doi.org/10.1016/j.rser.2018.12.031
11. B. Marion et al., Measured and modeled photovoltaic system energy losses from snow for colorado and wisconsin locations, Sol. Energy **97**, 112 (2013). https://doi.org/10.1016/J.SOLENER.2013.07.029
12. M.B. Øgaard et al., Identifying snow in photovoltaic monitoring data for improved snow loss modeling and snow detection, Sol. Energy **223**, 238 (2021). https://doi.org/10.1016/J.SOLENER.2021.05.023
13. A. Singh, D. Jones, Snow shedding properties of bifacial pv panels, in *2022 IEEE 49th Photovoltaics Specialists Conference (PVSC)* (IEEE, 2022), pp. 0646–0648. https://doi.org/10.1109/PVSC48317.2022.9938947
14. D. Riley, C. Hansen, J. Stein, M. Lave, J. Kallickal, B. Marion, F. Toor, A performance model for bifacial pv modules, in *2017 IEEE 44th Photovoltaic Specialist Conference (PVSC)* (IEEE, 2017), pp. 3348–3353. https://doi.org/10.1109/PVSC.2017.8366045
15. B. Marion, S. MacAlpine, C. Deline, A. Asgharzadeh, F. Toor, D. Riley, J. Stein, C. Hansen, A practical irradiance model for bifacial pv modules, In *2017 IEEE 44th Photovoltaic Specialist Conference (PVSC)* (IEEE, 2017), pp. 1537–1542. https://doi.org/10.1109/PVSC.2017.8366263
16. X. Sun, M.R. Khan, C. Deline, M.A. Alam, Optimization and performance of bifacial solar modules: a global perspective, Appl. Energy **212**, 1601 (2018)
17. A. Asgharzadeh, F. Toor, B. Bourne, M.A. Anoma, A. Hoffman, C. Chaudhari, S. Bapat, R. Perkins, D. Cohen, G. M. Kimball, D. Riley, A benchmark and validation of bifacial pv irradiance models, in *2019 IEEE 46th Photovoltaic Specialists Conference (PVSC)* (IEEE, 2019), pp. 3281–3287. https://doi.org/10.1109/PVSC40753.2019.8981272
18. S. Ghafiri, M. Darnon, A. Davigny, J.P. Trovao, D. Abbes, A comparative study of existing approaches for modeling the incident irradiance on bifacial panels, in *Electrimacs, Nancy, France* (2022). https://hal.archives-ouvertes.fr/hal-03831357
19. F. Brihmat, S. Mekhtoub, Pv cell temperature/pv power output relationships homer methodology calculation, in *Conférence Internationale des Energies Renouvelables* (CIER'13/International Journal of Scientific Research & Engineering Technology, International Publisher & C. O, 2014), Vol. 1
20. I. Reda, A. Andreas, Solar position algorithm for solar radiation applications, Sol. Energy **76**, 577 (2004). https://doi.org/10.1016/J.SOLENER.2003.12.003

21. S.A. Pelaez, C. Deline, bifacial_radiance: a python package for modeling bifacial solar photovoltaic systems, J. Open Source Softw. **5**, 1865 (2020). https://doi.org/10.21105/joss.01865
22. H.K. Seidlitz, S. Thiel, A. Krins, H. Mayer, Solar radiation at the earth's surface **3**, 705 (2001). https://doi.org/10.1016/S1568-461X(01)80071-5
23. M.A. Anoma, D. Jacob, B.C. Bourne, J.A. Scholl, D.M. Riley, C.W. Hansen, View factor model and validation for bifacial pv and diffuse shade on single-axis trackers, in *Sun Protection in Man* (Elsevier, Comprehensive Series in Photosciences, 2001), Vol. **3**, pp. 705–738. https://doi.org/10.1109/PVSC.2017.8366704
24. J.M. Bright, Solcast: validation of a satellite-derived solar irradiance dataset, Sol. Energy **189**, 435 (2019). https://doi.org/10.1016/j.solener.2019.07.086
25. L. Khalil, K.L. Bhatti, M.A.I. Awan, M. Riaz, K. Khalil, N. Alwaz, Optimization and designing of hybrid power system using homer pro, Mater. Today: Proc. **47**, S110 (2021). https://doi.org/10.1016/j.matpr.2020.06.054
26. A.S. Irshad, G.A. Ludin, H. Masrur, M. Ahmadi, A. Yona, A. Mikhaylov, N. Krishnan, T. Senjyu, Optimization of grid-photovoltaic and battery hybrid system with most technically efficient pv technology after the performance analysis, Renew. Energy **207**, 714 (2023). https://doi.org/10.1016/j.renene.2023.03.062
27. D. Abbes, A. Martinez, G. Champenois, Life cycle cost, embodied energy and loss of power supply probability for the optimal design of hybrid power systems, Math. Comput. Simul. **98**, 46 (2014). https://doi.org/10.1016/j.matcom.2013.05.004

Cite this article as: Soufiane Ghafiri, Maxime Darnon, Arnaud Davigny, João Pedro F. Trovão, Dhaker Abbes, A comprehensive performance evaluation of bifacial photovoltaic modules: insights from a year-long experimental study conducted in the Canadian climate, EPJ Photovoltaics **15**, 28 (2024)